

# Sol-gel synthesis of cuprous halide nanoparticles in a glassy matrix and their characterization

Ganesh Suyal,\*† Martin Mennig and Helmut Schmidt

Institut für Neue Materialien, Im Stadtwald, Gebäude-43, D-66123 Saarbrücken, Germany.  
E-mail: ganesh.suyal@epfl.ch

Received 25th March 2003, Accepted 16th May 2003

First published as an Advance Article on the web 30th May 2003

A sol-gel route to synthesize semiconductor cuprous halide CuX (X = Cl, Br) nanoparticles in a glassy matrix has been developed. Cu<sub>2</sub>O and HCl or HBr were used as the precursors for CuX and the matrix was prepared from 3-glycidoxypropyl trimethoxysilane (GPTS)/tetraethoxysilane (TEOS). Samples were dip-coated and cured either by ultraviolet (UV) irradiation at a temperature of 150 °C or in an oven at temperatures of 150–250 °C. Thin films (thicknesses 0.7–1.0 µm) containing cubic CuCl and CuBr nanoparticles with diameters ranging from 4–16 nm and 2–28 nm, respectively, were obtained. The ultraviolet-visible (UV-Vis) absorption spectra recorded at room temperature exhibited peaks at 371 and 379 nm for CuCl and at 410 and 391 nm for CuBr, corresponding to the Z<sub>1,2</sub> and Z<sub>3</sub> excitons respectively. X-Ray diffraction patterns showed the characteristic (111), (220) and (311) peaks of cuprous halides. High resolution transmission electron microscopy (HR-TEM) characterization proved that the lattice plane spacings correspond to copper halide nanocrystals.

## Introduction

Recently, glass like thin films containing semiconductor nanocrystals have drawn significant scientific attention due to their non-linear optical properties.<sup>1–4</sup> A lot of research has been conducted ever since Jain and Lind<sup>5</sup> first observed high optical non-linearity in CdS<sub>x</sub>Se<sub>1-x</sub> doped glasses. Most of the studies cover limited materials like CdS<sub>x</sub>Se<sub>1-x</sub>, CdTe, GaAs and CdS, with very low concentrations of nanocrystals.

Sugimoto *et al.*<sup>6</sup> prepared cuprous halide doped sodium aluminoborosilicate glasses and achieved growth of quantum dots under controlled heat treatment conditions. Nogami *et al.*<sup>7</sup> have applied the sol-gel method to synthesize bulk glasses containing CuCl and CuBr nanocrystals. For this, a suspension of CuCl/CuBr was re-precipitated at high temperatures (800–900 °C) to obtain cubic copper halide particles. Kriltz *et al.*<sup>8</sup> have synthesized sol-gel glasses containing cuprous halide microcrystals for photochromic applications. Yoon *et al.*<sup>9</sup> have studied the effect of phase separation on the precipitation of CuCl quantum dots in sodium borosilicate glasses. Kraevskii and Solinov<sup>10</sup> have prepared glasses containing CuCl microcrystals and studied the thermochromic effect in those glasses.

Besides their other applications, these glasses can also be seen as future optical filters due to their sharp UV-absorption edge. Filters, which would completely block UV radiation in the visible light, would be of significant technological importance and it is known that the exciton absorption peaks of Cu-halide nanoparticles fall very close to the UV-Vis boundary.

Such filter glasses containing semiconductor nanoparticles with a sharp absorption edge are commercially available and produced by Corning<sup>11</sup> and Schott<sup>12</sup> by the melting method. This method requires temperatures as high as 1300–1400 °C and special melting equipment and facilities, due to the high concentration of volatile halide compounds. This complicated melting process makes these filters costly and thus limits their applicability to large areas. The investigation of sol-gel materials as new and cheaper alternatives for the coating of glass substrates has also proceeded at a rapid pace over the last

few years. Sol-gel materials can be particularly suitable alternatives to synthesize thin films containing copper halide nanoparticles. However, the presence of water in the sol and gel can easily shift the Cu<sup>2+</sup>/Cu<sup>+</sup> equilibrium mainly to Cu<sup>2+</sup>, thus making it difficult to prepare films containing monovalent copper exclusively.

Therefore, the aim of the present work was to develop a sol-gel synthesis route to organic-inorganic coatings containing CuCl and CuBr nanocrystals on glass substrates by finding a suitable mechanism for the stabilization of copper ions in the Cu<sup>+</sup> state during the sol synthesis and coating formation process. After that the CuCl and CuBr nanoparticles should be characterized precisely (size, crystallinity, optical properties).

## Experimental

To synthesize thin films containing CuCl/CuBr nanoparticles, the matrix sol used was prepared from a precursor solution with the molar ratios GPTS:TEOS:water:alcohol = 1:1:2:9. The GPTS-TEOS system was chosen; since it is known from the literature<sup>13</sup> that its short chain organic groups can be burnt off without any cracking of coatings.

To synthesize GPTS/TEOS sols with a GPTS:TEOS molar ratio of 1:1, a mixture of 120 ml ethanol, 100 ml GPTS and 100 ml TEOS was taken in a 500 ml round bottomed flask connected to a water condenser and heating arrangement. After heating at 80 °C for 0.5 h, 28.5 ml of 0.1 molar HNO<sub>3</sub> solution was added dropwise to it within 3–4 min. This mixture was reacted for 24 h under the same conditions at 80 °C and finally 120 ml more ethanol was added to it. After reacting it for 0.5 h at 80 °C, the resulting sol was cooled down to room temperature. The sol synthesized this way was very stable at room temperature and could be stored for more than a year without gelation.

To synthesize thin films containing CuCl nanoparticles, 0.60 g cuprous oxide (Cu<sub>2</sub>O) was mixed with 7.5 ml of acetonitrile using an ultrasonic bath for 5 min. In another glass container 17.5 ml of pre-hydrolyzed GPTS-TEOS sol was taken. The cuprous oxide suspension was added dropwise to the GPTS-TEOS sol and stirred at 25 °C for 30 min. Finally 3.0 ml of hydrochloric acid (Fluka 37%) was added to it

†Present address: Federal Institute of Technology, EPFL, IMX-LC, Ecublens, CH-1015 Lausanne, Switzerland.

dropwise and stirred for 48 h. To synthesize a sol containing copper bromide, 0.30 g cuprous oxide was mixed with 7.5 ml acetonitrile, followed by the addition of 3.0 ml of HBr (Aldrich 48%), and the rest of the process was kept the same as described above.

Pre-washed (with Helmanex solution) soda-lime and fused silica glass substrates were dip-coated with a lifting speed of 4–6 mm s<sup>-1</sup>. Samples were dried at 60 °C for 15 min in a drying oven and curing was carried out either in an oven at temperatures between 150 °C and 250 °C for 30 min or in a UV-IR beltron machine (1200 W and 150 °C) for 4 min.

To investigate the optical properties, UV-Vis absorption spectra of the films coated on the glass slides were recorded with an OMEGA 30 UV-Vis spectrometer (Bruins Instrument). For carrying out low temperature UV-Vis measurements, a VARIAN CARY 5E spectrophotometer was used. Extinction spectra of thin films were measured at liquid nitrogen temperature ( $T = 84$  K) and at a pressure of  $5 \times 10^{-4}$  mbar. The UV-Vis spectra were recorded at wavelengths ranging from 300 to 1000 nm. The thickness of the films was measured with a profilometer (diamond stylus, nanosurf). To obtain information about the crystalline phase and the size of the cuprous halide nanoparticles, an X-ray spectrometer (SIEMENS D500, 40 kV, 35 mA,  $\text{CuK}_\alpha = 1.5405 \text{ \AA}$ ) with a LiF monochromator was used. The diffracted X-rays were collected by scanning between  $2\theta = 20\text{--}60^\circ$  in  $0.04^\circ$  steps.

To perform the electron microscopic characterization of the copper halide nanocrystals in the films, a JEOL 200 CX high-resolution transmission electron microscope (HR-TEM) was used. The samples were prepared by scratching off splinters from the copper halide containing coatings. This scratched material was deposited onto a carbon coated copper grid and was investigated using HR-TEM.

## Results and discussion

Copper(I) oxides are known to be soluble in strong acids or strong bases only. Hence, the chlorination/bromination of copper(I) ions was done by incorporating HCl/HBr to the sol containing cuprous precursor. The addition of halide ions greatly increases the solubility of the cuprous salts due to the formation of halocuprate(I) anions<sup>14</sup> of the type  $\text{CuX}_2^-$  and  $\text{CuX}_3^{2-}$  resulting in a green colored and transparent solution. Therefore, the suspension of cuprous oxide in acetonitrile was mixed with the matrix sol and the chloride ions were added to it to get a clear and transparent solution. Since the stability of the cuprous ions relative to that of cupric ions may be affected by the solvent, acetonitrile, in which  $\text{Cu}^+$  is more stable than  $\text{Cu}^{2+}$ ,<sup>15</sup> acetonitrile was chosen as a solvent.

Colorless transparent coatings with thicknesses from 0.8–1.0  $\mu\text{m}$  were obtained by a single deposition process after heat treatment in a UV-IR beltron machine connected to a low pressure Hg–Xe lamp (1200 W) and IR irradiation (150 °C).

### UV-Vis characterization

**CuCl nanoparticles.** To investigate the optical properties of thin films containing CuCl nanoparticles and to understand the mechanism of their formation in thin films, the UV-Vis spectra of the samples were measured at various intervals of the curing procedure. Fig. 1 shows the UV-Vis spectra of thin films containing CuCl nanoparticles after drying for 30 min at 60 °C and for different time periods of treatment in the UV-IR irradiation.

Fig. 1, curve d, closely resembles the reported absorption spectra of cuprous chloride.<sup>16</sup> Peaks at 371 and 381 nm can be attributed to copper chloride nanoparticles, which are termed as  $Z_3$  and  $Z_{1,2}$  resulting from the excitation associated with two spin orbital valence sub-bands. The  $Z_3$  line originates from the

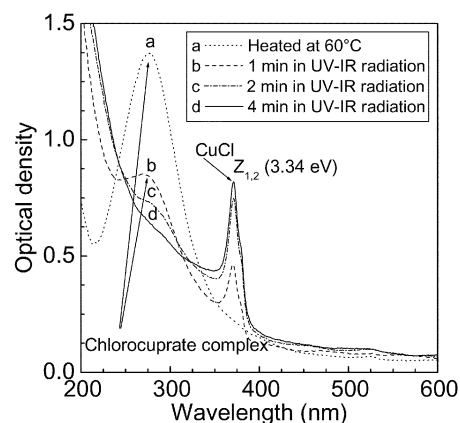


**Fig. 1** Stepwise generation of CuCl nanocrystals under different heat treatment conditions: (a) in an oven, 30 min, 60 °C; and in a UV-IR (1200 W, 150 °C) beltron machine for (b) 1 min, (c) 2 min, (d) 4 min.

two-fold degenerate sub-band  $\Gamma_6$ , and the  $Z_{1,2}$  line originates from the four fold degenerate valence sub-band  $\Gamma_8$ .<sup>17</sup>

The sample dried at 60 °C shows only one broad peak at 280 nm (Fig. 1, curve a), which can be attributed to the chlorocuprate anions.<sup>18</sup> After curing for 1 min with UV-IR radiation a new peak is obtained at 371 nm, resulting in the decrease of the intensity of the peak at 280 nm (Fig. 1, curve b). The same trend is obtained after UV-IR treatment for 2 min, as one can see from Fig. 1, curve c. The curing of the same sample for 4 min in a beltron machine generated an intense characteristic peak of cuprous chloride at 371 nm, and complete disappearance of the peak at 280 nm (Fig. 1, curve d). No further change in absorption spectra was observed on curing the samples for longer time periods (6 to 10 min).

**CuBr nanoparticles.** In order to investigate the optical properties of thin films containing cuprous bromide nanoparticles and to follow the generation of CuBr nanoparticles during UV-IR treatment, the absorption spectra of the samples were recorded after 1, 2, and 4 min of UV-IR treatment. Fig. 2 shows the UV-Vis spectra of thin films containing CuBr nanoparticles, measured at room temperature. In Fig. 2, curve d closely resembles that reported in the literature<sup>7</sup> and the peaks at 391 nm and 410 nm can be attributed to cuprous bromide nanoparticles.

The sample dried at 60 °C shows a broad peak at 310 nm corresponding to bromocuprate complexes,<sup>18</sup> and two very weak peaks at 390 nm and 410 nm, characteristic of CuBr (Fig. 2, curve a). On exposing the samples to UV-IR irradiation, the intensity of the peak at 310 nm decreases and the

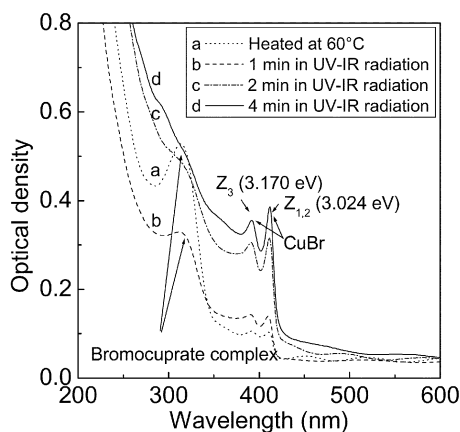
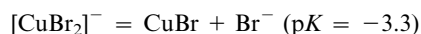


**Fig. 2** Stepwise generation of CuBr nanocrystals under different heat treatment conditions: (a) in an oven, 30 min, 60 °C; and in a UV-IR beltron machine (1200 W, 150 °C) for (b) 1 min, (c) 2 min, (d) 4 min.

intensity of cuprous bromide absorption peaks at 390 nm and 410 nm increases, as one can see from curves b and c in Fig. 2. The intensity of the absorption peak becomes constant after 4 min of UV-IR treatment (Fig. 2, curve d). Unlike cuprous chloride (Fig. 1), cuprous bromide exciton peaks can be seen even for the samples heat treated in an oven at 60 °C, whereas in the case of cuprous chloride the absorption peak appeared only after UV-IR treatment of the samples. As is known from the literature,<sup>19</sup> the dissociation constant ( $pK$ ) for the  $[\text{CuBr}_2]^-$  complex, which gives the following dissociation products, is  $-3.3$ :



Therefore, the soluble bromocuprate complex, unlike the chlorocuprate complex, dissociates to copper bromide even at 60 °C, resulting in a CuBr absorption peak in the UV-Vis absorption spectra (Fig. 2, curve a).

From these observations it can be concluded that the addition of halide ions to a suspension containing  $\text{Cu}_2\text{O}$  results in acid soluble halocuprate complex ions. The addition of HCl results in dichlorocuprate(i) and trichlorocuprate(i) anions, showing an absorption at 275 nm for chlorocuprate anions, whereas, the addition of HBr results in dibromocuprate(i) and tribromocuprate(i) anions showing an absorption at 310 nm for bromocuprate anions (Fig. 1 and Fig. 2, curve a).<sup>18</sup> During the UV-IR treatment, these acid soluble halocuprate complexes were decomposed to form CuCl and CuBr in the  $\text{SiO}_2$  films.

After the synthesis route had been developed successfully, the CuCl and CuBr nanoparticles should now be characterized with respect to their size and crystallinity. The size of the copper halide particles was determined from the absorption spectra and then compared to the results obtained by XRD and HR-TEM. Ekimov *et al.*<sup>20</sup> reported an equation relating the particle radius ( $r$ ) and the lowest energy ( $E$ ) of the confined  $Z_3$  exciton in UV-Vis spectra as:

$$E = E_g - E_{\text{ex}} + 0.67 \frac{\hbar^2 \pi^2}{2M_s r^2}$$

where  $E_g - E_{\text{ex}}$  is the  $Z_3$  exciton energy for the bulk crystal (3.218 eV for CuCl and 3.125 eV for CuBr, at liquid nitrogen temperature)  $\hbar$  is Planck's constant divided by  $2\pi$  and  $M_s$  is the translational mass ( $M_s = 1.9 m_0$ , where  $m_0$  is the free electron mass).

In order to apply this equation to calculate the particle size by the position of the  $Z_3$  exciton energy, UV-Vis spectra of thin films containing CuCl and CuBr nanoparticles were recorded. The absorption spectra measured at 88 K are shown in Fig. 3. The spectra were recorded at liquid nitrogen temperature

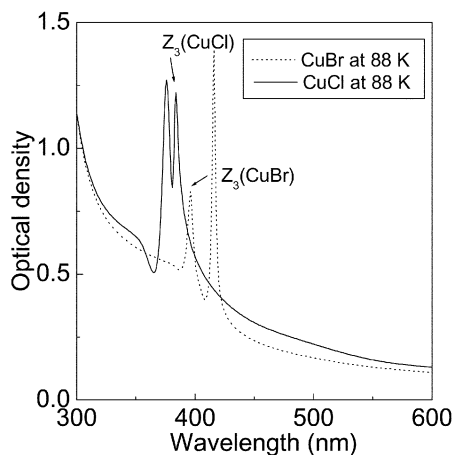


**Fig. 3** UV-Vis absorption spectra of thin films containing CuCl and CuBr nanoparticles recorded at 88 K.

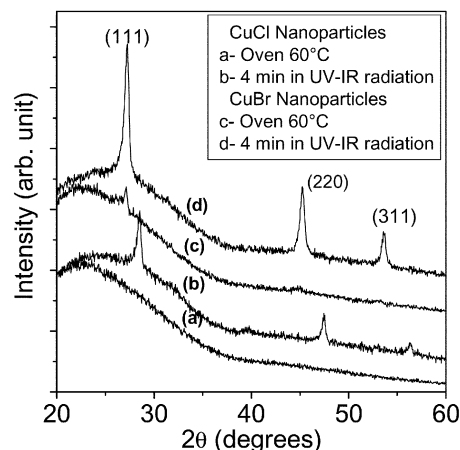


**Fig. 4** XRD patterns of thin films containing CuCl nanoparticles (a) dried in an oven at 60 °C, 30 min, (b) UV-IR treatment, 4 min; thin films containing CuBr nanoparticles (c) dried in an oven at 60 °C, 30 min, (d) UV-IR treatment, 4 min.

(88 K), because the  $Z_3$  exciton peak is not visible at room temperature for CuCl and the  $Z_3$  exciton energies for the cuprous halide bulk crystals are known at liquid nitrogen temperature only. Subsequently, the particle size was determined using the observed positions of the  $Z_3$  peaks from the measured spectra using the above equation. The particle diameters “ $2r$ ” were calculated equal to 10.0 nm for CuCl and 12.0 nm for CuBr.

#### X-Ray diffraction characterization

**CuCl nanoparticles.** In order to confirm the crystalline behavior of the nanoparticles and the phase in which these particles exist in the films, X-ray diffraction measurements were carried out. The X-ray diffraction patterns of the film containing CuCl nanoparticles are shown in Fig. 4, curve b.

XRD patterns observed are in very good agreement with the literature values and three characteristic peaks are of cuprous chloride.<sup>21</sup> The most intense peak corresponding to the (111) plane is centered at 28.55°, while two other less intense peaks corresponding to the (220) and (311) planes are centered at 47.47 and 56.33° respectively. A comparison between the literature reported and experimentally observed X-ray diffraction peak positions and their intensities is shown in Table 1. The observed X-ray diffraction pattern indicates that the cuprous chloride is present as a nanokite phase (powder diffraction file no. 6-344) in thin films.

The stepwise generation of cuprous chloride nanoparticles with respect to the change in heat treatment conditions was followed by using the X-ray diffraction technique also. The measured X-ray diffraction patterns are shown in Fig. 4, curves a and b. It can be seen that for the samples heated at 60 °C in an oven, no X-ray diffraction peak was observed (Fig. 4, curve a), indicating the absence of CuCl in the thin film after heating the sample at 60 °C for 15 min. The same behavior was also shown by UV-Vis spectra. The sample treated with UV-IR irradiation (1200 W, 150 °C) for 4 min shows all the three diffraction peaks

**Table 1** A comparison of experimentally observed and literature reported X-ray diffraction peak positions and intensities for nanokite CuCl

Plane (hkl)	Literature data for CuCl <sup>21</sup>		Experimental data for CuCl	
	2θ	Intensity	2θ	Intensity
111	28.52	100	28.55	100
220	47.43	55	47.47	52
311	56.29	30	56.33	27

**Table 2** The diameters of CuCl nanoparticles as measured using the Scherrer equation, UV-Vis spectra and HR-TEM analysis (measurement error is  $\pm 10\%$ )

Scherrer equation '2r'	UV-Vis spectra '2r'	HR-TEM '2r'
11 nm	10 nm	12 nm

corresponding to the (111), (220) and (311) planes of the CuCl nantokite phase (Fig. 4, curve b).

From the angle corresponding to the maximum diffraction (here the 111 peak) and the half-width of the diffraction peak, the size of the nanoparticles was calculated using the Scherrer equation. The half width of the peak was measured to be equal to  $0.935^\circ$ , and  $2\theta$  was measured equal to  $27.20^\circ$ . Using these parameters, a particle diameter of 11.0 nm was determined. Since this is in very good agreement with the results of the spectroscopic method (see above), it can be concluded that the vast majority of the nanoparticles are single crystals.

Table 2 shows the size of the CuCl nanoparticles calculated using the Ekimov equation (peak position in UV-Vis spectra), the Scherrer equation, and HR-TEM analysis. The particle sizes determined by the three different methods compare well. The lattice constant was calculated to be equal to  $5.42 \text{ \AA}$  using the X-ray diffraction pattern, which also is in good agreement with the literature reported value for CuCl.<sup>22</sup>

**CuBr nanoparticles.** The X-ray diffraction pattern of the thin film containing CuBr nanoparticles is shown in Fig. 4, curve d. The XRD patterns observed are in good agreement with the literature values for CuBr and the observed peaks can be attributed to the cuprous bromide  $\gamma$ -phase.<sup>23</sup> The most intense peak corresponding to the (111) plane is centered at  $27.26^\circ$ , while two other less intense peaks corresponding to the (220) and (311) planes are centered at  $45.07^\circ$  and  $53.54^\circ$  respectively. A comparison between the experimental and the literature reported X-ray diffraction peak positions and intensities is shown in Table 3. Therefore, it can be said that the observed X-ray diffraction pattern was found to be in good agreement with the  $\gamma$ -CuBr patterns, indicating that the cuprous bromide is present as the  $\gamma$ -phase in these thin films.

The stepwise generation of cuprous bromide nanoparticles with the change in heat treatment conditions was also followed by recording the X-ray diffraction patterns after every step of heat treatment. The recorded X-ray diffraction patterns are shown in Fig. 4, curves c and d. It is clear from the figure that for the sample heated at  $60^\circ\text{C}$  in an oven, only one diffraction peak corresponding to the (111) plane is observed (Fig. 4, curve c), whereas no diffraction peaks were observed corresponding to the (220) and (311) planes. It shows that a small amount of CuBr has already been formed after heating the sample at  $60^\circ\text{C}$  for 15 min. This result is in good agreement with the UV-Vis spectra. For the sample treated for 4 min in UV-IR irradiation, all three diffraction peaks corresponding to  $\gamma$ -CuBr are clearly visible (Fig. 4, curve d).

The particle diameter '2r' for CuBr nanoparticles was determined to be equal to 12 nm using the Scherrer equation. For comparison, the particle sizes measured using the three

**Table 3** A comparison of experimentally observed and literature reported X-ray diffraction peak positions and intensities for  $\gamma$ -CuBr

Plane (hkl)	Literature data for CuBr <sup>23</sup>		Experimental data for CuBr	
	$2\theta$	Intensity	$2\theta$	Intensity
111	27.12	100	27.26	100
220	45.02	50	45.07	51
311	53.34	35	53.54	32

**Table 4** The diameters of CuBr nanoparticles as measured using the Scherrer equation, UV-Vis spectra and HR-TEM analysis (measurement error is  $\pm 10\%$ )

Scherrer equation '2r'	UV-Vis spectra '2r'	HR-TEM '2r'
12 nm	12 nm	14 nm

different methods are listed in Table 4. The particle sizes measured by the different methods are in good agreement. The lattice constant was calculated to be equal to  $5.68 \text{ \AA}$  using the X-ray diffraction pattern, which also is in good agreement with the literature reported value for CuBr.<sup>22</sup>

#### Stability of CuCl nanoparticles in different atmospheres.

After storage of the cuprous halide samples in air, a decrease in the intensity of the characteristic cuprous halide absorption peak was observed, which vanishes completely after a few days. Therefore, the stability of CuCl in the thin films was studied in different atmospheres. The change in the area of the  $Z_{1,2}$  absorption peak for CuCl nanoparticles after different time periods is shown in Fig. 5 for samples stored in air, in a desiccator (exclusion of moisture) and in vacuum.

This figure shows that the CuCl peak vanishes completely in air within 10 days, on the other hand for the samples stored in a desiccator (exclusion of moisture) a relatively small decrease in the intensity of absorption peak was observed after 56 days. A decrease in the peak intensity can be observed in vacuum as well, though it is very small. As exclusion of moisture drastically increases the stability of CuCl, it can be said that CuCl is very sensitive towards moisture.

The possible explanation for this behavior is the unstable nature of cuprous chloride. In the presence of moisture and air, CuCl is known to be oxidized and hydrolyzed to a green product that approaches copper(II) chloride dihydroxide ( $\text{CuCl}_2 \cdot 3\text{Cu}(\text{OH})_2$ ).<sup>24</sup> In order to confirm the transformation of Cu(I) into Cu(II), X-ray diffraction patterns of freshly prepared thin films and films after exposure to air at  $25^\circ\text{C}$  for 3 weeks were measured and are shown in Fig. 6. A remarkable change in the XRD patterns can be observed from this figure. The samples exposed to air at  $25^\circ\text{C}$  for 3 weeks exhibit XRD peaks corresponding to copper(II) chloride dihydroxide.<sup>25</sup> Therefore, XRD measurements also support the oxidation of Cu(I) into Cu(II).

**Effect of post heat treatment: CuCl nanoparticles in thin films.** During the heat treatment of the samples containing CuCl, at higher temperatures ( $>200^\circ\text{C}$ ) in an oven, it was observed that the intensity of CuCl exciton peaks decreases and

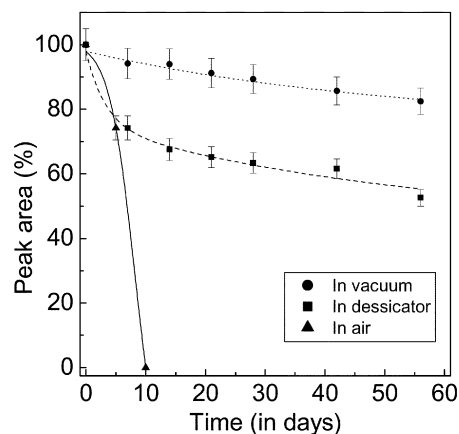


**Fig. 5** The change in the area of the  $Z_{1,2}$  absorption peak of CuCl in different atmospheres, as a function of time (in days).

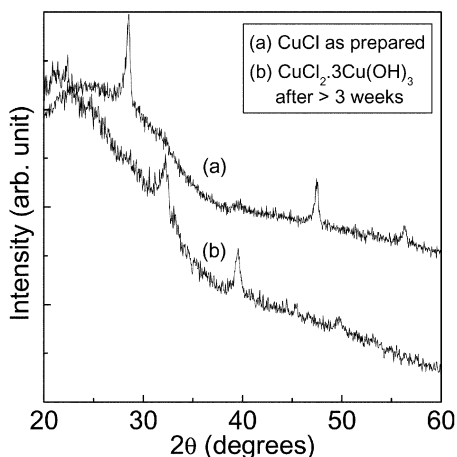
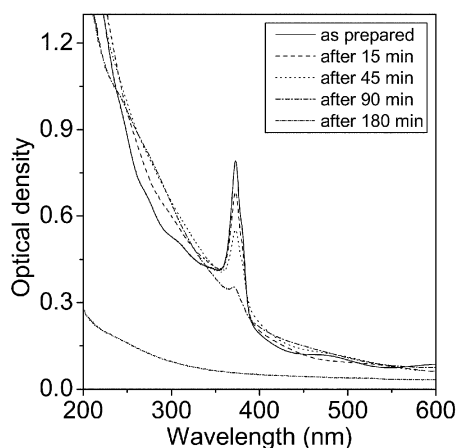


**Fig. 6** XRD patterns of thin films containing CuCl nanocrystals (a) as prepared, (b) on exposure to air at 25 °C for three weeks.

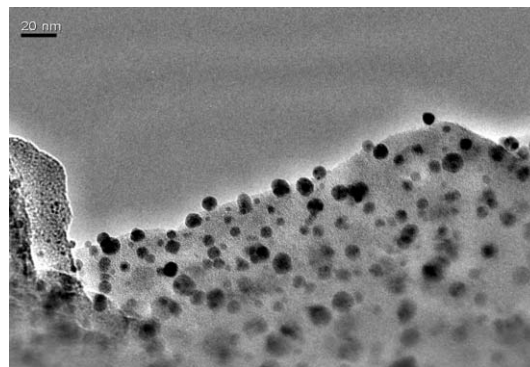
disappears completely after a certain time period. To understand the mechanism, CuCl containing samples were heated at 250 °C in an oven for different time periods and their measured UV-Vis spectra are shown in Fig. 7.

Fig. 7 clearly shows that on heating the samples at 250 °C in air for 15 min, there is a small decrease in the intensity of the UV-Vis absorption peak, whereas a remarkable decrease in the intensity can be observed after 45 min. After 3 h of heat treatment at 250 °C in air the characteristic absorption peak due to CuCl completely disappears, indicating that there is no CuCl left in the films after 3 h. Simultaneously, a strong absorbance in the UV range (200–300 nm) was observed that may be attributed to the decomposed organics in the coatings. It initially increases till 45 min of heating and remarkably decreases after 3 h of heating.

It has been shown in the above sections that  $\text{Cu}^+$  is very unstable and oxidizes to  $\text{Cu}^{2+}$  in air. Therefore, in order to understand the mechanism of the transformation during heat treatment of cuprous halides in an oven at 250 °C, two possibilities may be considered: 1) either cuprous chloride has been changed into a cupric compound with the formation of  $\text{CuCl}_2 \cdot 3\text{H}_2\text{O}$ , or 2) CuCl has been decomposed into  $\text{Cu}^+$  and  $\text{Cl}^-$ . If there is  $\text{CuCl}_2 \cdot 3\text{H}_2\text{O}$  in the films it should show crystalline behavior. However, the X-ray diffraction measurement of the sample heated at 250 °C for 3 h shows non-crystalline behavior, indicating the decomposition of CuCl into  $\text{Cu}^+/\text{Cu}^{2+}$  and  $\text{Cl}^-$ . If copper is still present in the films as ionic copper, it should form copper colloids under a reducing



**Fig. 7** UV-Vis absorption spectra of thin films containing CuCl nanocrystals on heating at 250 °C in air for different time periods: as prepared, and after 15 min, 45 min, 90 min and 180 min.



**Fig. 8** HR-TEM image showing the CuCl nanoparticles dispersed in the glass matrix.

atmosphere. Therefore, the samples exposed to air for 3 weeks were heat-treated under a reducing atmosphere ( $\text{N}_2/\text{H}_2 = 92/8$ ,  $80 \text{ l h}^{-1}$ ) at 450 °C for 1 h with a heating rate of  $100 \text{ K h}^{-1}$ . The formation of copper colloids was followed by UV-Vis absorption spectroscopy, which shows only one absorption peak at  $587 \text{ nm}^{26}$  indicating the formation of copper colloids in the thin films. This result supports the presence of copper in ionic form in the films. The same observations were made for the thin films containing CuBr nanoparticles also.

#### HR-TEM characterization

In order to determine the size and structure of the CuX ( $X = \text{Cl}, \text{Br}$ ) nanoparticles by an alternative way, high-resolution electron microscopy (HR-TEM) was carried out. The HR-TEM micrographs of the samples containing CuCl nanoparticles are shown in Fig. 8 and Fig. 9. CuCl particles of diameters ranging from 4–16 nm (average diameter = 12 nm) dispersed in the glass-like matrix are visible in Fig. 8. A single particle having a diameter of 8 nm and embedded in the matrix is shown at higher magnification in Fig. 9a.

For the samples heat treated in a beltron machine, the particles formed are well separated and uniformly dispersed, whereas, the samples heated in an oven for a long time (150 °C,

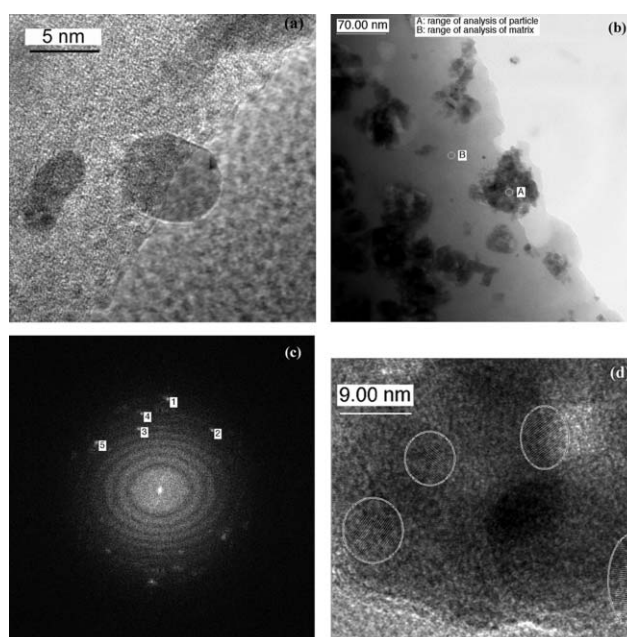


**Fig. 9** (a) High resolution TEM image of a single CuCl particle embedded in glass matrix, (b) HR-TEM image of some agglomerated particles, (c) electron diffraction pattern of a small region selected from the agglomerates, (d) the spots in the electron diffraction pattern are probably formed from the marked nanocrystals.

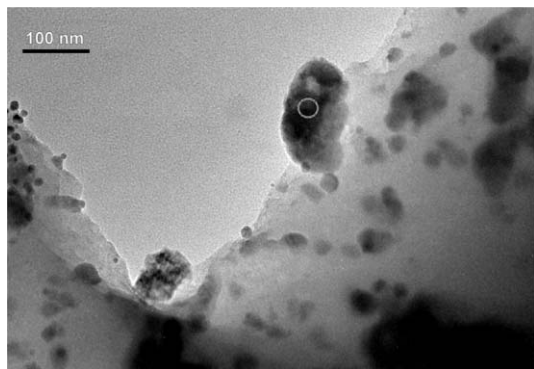


Fig. 10 HR-TEM image of a thin film containing CuBr nanoparticles.

2 h) showed the formation of some agglomerates. Fig. 9b shows a HR-TEM picture of a selected region containing some agglomerates. In order to see what these agglomerates are formed of, their electron diffraction pattern was recorded and is shown in Fig. 9c.

The analysis of the electron diffraction pattern yields the following distances: 2.02 Å corresponding to the (111) plane of Cu, 2.34 Å, 2.36 Å, 2.35 Å, corresponding to the (200) plane of CuCl and 2.87 Å corresponding to the (111) plane of CuCl. A lattice plane measurement of these particles indicates that the films consist still of the nantokite phase of cuprous chloride. The observation of these lattice spacing suggests that the big clusters were due to the agglomeration of small CuCl particles. In Fig. 9d, probable nanocrystals are imaged using probable CuCl spots of the diffractogram and applying the Fourier fittings. The investigated particles, which are marked by circles, possess diameter of the order of 8 nm (6–9 nm). The high-resolution micrograph of the sample heated at 200 °C for 2 h indicates the formation of clusters of 70–80 nm in size, which can again be explained by the agglomeration of small CuCl nanoparticles on holding the sample at 200 °C for 2 h.

Apart from CuCl, lattice spacing measurements show the spacings corresponding to Cu planes also, hence copper is also present in the agglomerates. As the UV-Vis spectra do not show any absorption peak corresponding to a copper plasmon peak, it is very probable that the formation of copper is induced by the incidence of the electron beam on the CuCl particles during HR-TEM investigations.

The HR-TEM image of a thin film containing CuBr nanocrystals is shown in Fig. 10. This figure shows that in the case of CuBr, the nanoparticles are not uniform and some agglomerates are also formed. Particles with diameters ranging from 2–28 nm (average diameter = 14 nm) are formed.

## Conclusions

The sol–gel process has successfully been used for the synthesis of organic–inorganic thin films containing CuX (X = Cl, Br) nanoparticles. Copper could be stabilized in the Cu<sup>+</sup> state as acid soluble halocuprate complexes in solution, in the presence of acetonitrile. These complexes decompose during heat treatment to form copper halide nanoparticles. The formation of acid soluble halocuprate complexes like CuX<sub>2</sub><sup>-</sup> and CuX<sub>3</sub><sup>2-</sup>

(X = Cl, Br) and their decomposition during the heat treatment to CuCl and CuBr was confirmed by UV-Vis spectroscopy, which showed high intensity Z<sub>1,2</sub> and Z<sub>3</sub> exciton peaks thus confirming the formation of cuprous halide nanocrystals. The thin films containing CuCl and CuBr were also characterized by X-ray diffraction technique. For cuprous chloride and cuprous bromide samples, particles with average diameters of 11 nm and 14 nm respectively, were formed after heat treatment at 150 °C in a UV-IR beltron machine. Cubic nantokite and γ phases were observed for CuCl and CuBr nanoparticles respectively.

## Acknowledgements

The authors want to thank Dr. U. Werner for carrying out the TEM measurements, and the State of Saarland, Germany, for financial support.

## References

- 1 L. E. Brus, *Appl. Phys.*, 1992, **A53**, 465–474.
- 2 P. Gillot, J. C. Merle, R. Levy, M. Robino and B. Hönerlage, *Appl. Phys.*, 1991, **B153**, 403.
- 3 Y. Kondo, Y. Kuroiwa, N. Sugimoto, T. Manabe, S. Ito, T. Tokizaki and A. Nakamura, *J. Non-Cryst. Solids*, 1996, **196**, 90.
- 4 H. Ohmura and A. Nakamura, *Phys. Rev. B*, 1999, **59**(19), 12216.
- 5 R. K. Jain and R. C. Lind, *J. Opt. Soc. Am.*, 1983, **73**(5), 647.
- 6 N. Sugimoto, M. Yamamoto, T. Manabe and S. Ito, in *Proceedings of the International Conference on New Glasses*, Tokyo, October 16–17 1991.
- 7 M. Nogami, Y. Q. Zhu and K. Nagasaka, *J. Non-Cryst. Solids*, 1991, **134**, 71.
- 8 A. Kritz, R. Facht, M. Müller and H. Bürger, *J. Sol-Gel Sci. Technol.*, 1998, **11**(2), 197.
- 9 Y. K. Yoon, W. T. Han and S. J. Chung, *J. Non-Cryst. Solids*, 1996, **203**, 195.
- 10 S. L. Kraevskii and V. F. Solinov, *Glass Phys. Chem.*, 2001, **28**(1), 11.
- 11 Corning Glasses No. 2403 to 2434 and 3480 to 3486.
- 12 Schott Glasses No. R. G. 610 to RG 715 and OG 5515 to OG 5590.
- 13 M. Schmitt, Ph.D. Thesis, University of Saarland, Saarbrücken, Germany, 1998.
- 14 D. G. Peters and R. L. Caldwell, *Inorg. Chem.*, 1967, **6**, 1478.
- 15 F. A. Cotton and G. Wilkinson, *Advanced Inorganic Chemistry*, Wiley, New York, 3rd edn., 1971, p. 906.
- 16 K. Tsunetomo, R. Shimizu, A. Kawabuchi, H. Kitayama and Y. Osaka, *Jpn. J. Appl. Phys.*, 1991, **30**(4B), 764.
- 17 M. Cardona, *Phys. Rev.*, 1963, **129**(1), 69.
- 18 K. Sugasaka and A. Fujii, *Bull. Chem. Soc. Jpn.*, 1976, **49**(1), 82.
- 19 *Ullmann's Encyclopedia of Industrial Chemistry*, Wiley-VCH Verlag GmbH & Co KGaA, Germany, 1986, vol. A7, p. 587.
- 20 A. I. Ekimov, Al. L. Efros and A. A. Onushchenko, *Solid State Commun.*, 1985, **56**, 921.
- 21 Powder Diffraction File, Alphabetical Indexes for Experimental Patterns, Inorganic Phases, Sets 1-51, page 239, file no. 6-344.
- 22 L. Börnstein, *Numerical Data and Fundamental Relationship in Science and Technology, II-VI Compounds*, New Series III 17b, ed. O. Madelung, Springer Verlag, Berlin, 1982.
- 23 Powder Diffraction File, Alphabetical Indexes for Experimental Patterns, Inorganic Phases, Sets 1-51, page 239, file no. 6-292.
- 24 *Ullmann's Encyclopedia of Industrial Chemistry*, vol. A7, page 573.
- 25 Powder Diffraction File, Alphabetical Indexes for Experimental Patterns, Inorganic Phases, Sets 1-51, page 239, file no. 18-439.
- 26 G. Suyal, Ph.D. Thesis, INM Saarbrücken, Germany, 2002.